**CARDIFF UNIVERSITY**

**SCHOOL OF PHYSICS AND ASTRONOMY**

MSc Research Project

# Updating Gravitational Wave Constraints using Modified Gravity


Abhishek Karkola

Project Supervisor:

**Dr. Ian Harrison**

PXT999 Research Project

# Updating Gravitational Wave Constraints using Modified Gravity

Supervisor : Dr. Ian Harrison

Abhishek Karkola

2 September 2022

## Contents

# 1 Introduction

It is now widely acknowledged that General Relativity (GR) plays a significant role in the cosmological standard model and we also understand that GR is not a final theory. Although it is a good theory, it falls short at small scales, most notably when it comes to the issue of a cosmological constant. Any attempts to expand or alter GR to solve either of these drawbacks will lead to the formation of other gravitational theories since, under the assumption of Lorentz invariance, it has been the only coherent theory of a mass-less spin-2 field. Since this would fundamentally alter our understanding of gravity, it is important to keep an eye out for any indications of these new theories. Additionally, doing so is the most rigorous approach to constrain general relativity (GR). As well as complying to a set of theoretical constraints intended to ensure that one is working with a fundamentally sound theory space, they often involve only a small number of GR extensions and only introduce one new component. Due to the fact that the vast majority of scalar-tensor theories recognised in the literature are Horndeski theories and that their theory space is still only partially explained by a small number of interaction effects in the Lagrangian, such theories offer a similar rich and well-setup for constraining variances from GR and developing new gravitational theories.

Since gravity theory was created to modify General Relativity, the finding of gravitational waves (GWs) from GW170817 [1, 2], a binary neutron star, has had a tremendous impact on that system space (GR). The very modest discrepancy between the propagation speeds of light ($c$) and the speed of gravitational waves ($c_T$) was reduced to less than $10^{-15}$ by the detection of a gamma-ray equivalent at redshift zero, which occurred 1.7 seconds after the GW merger signal [3, 4]. This finding then links back to the modified gravity (MG) theories, which are also capable of predicting $c_T \neq c$. The quartic and quintic Galileon theories, subject to some very minor assumptions, fall into this category of theories that appear to be unable to satisfy $c_T = c$ across all redshifts and are thus ruled out. For some ranges of their internal parameters, various theories, including Generalized Proca theories and TeVeS [5, 6], can satisfy $c_T = c$. Another group of hypotheses, such as f(R) gravity [7], are not constrained by the GW170817 event because they are unaffected by the GW propagation speed. Given that GW170817 provides a specific piece of information at low redshift ($z = 0.01$) in terms of cosmological distance measurements, it is not unexpected that several hypotheses withstood this restriction.

We pay close attention to the following two research questions during the process:

- How much does it constrain on $\alpha_M$ Horndeski parameter (see section 2) by the inclusion of the GW event GW190521 as a standard siren.
- Constraints on coeficients apperaring on $\alpha_M$ and $\alpha_B$ Horndeski parameters and plotting the contours corresponding to constraints from LIGO-Virgo data.

The paper is laid out as follows: in Section 2, we explore the the horndeski gravity and its parameter; in Section 3, we introduce the methodology we followed for the research ; in Section 4, we introduce theoretical modelling; and in Section 5, we offer our findings; in section 6, we finally reach the conclusion and discuss the future prospects for this project. In Section 7.1, we discuss the critique of the project.

# 2 Précis of literature

The Galileon family, the KGB, the f(R) gravity, the DGP gravity, and many more well-known models are all included in the large group of known as horndeski gravity. Here, we utilise the Horndeski Lagrangian because it offers a practical yet adaptable framework for trying to include both EM constraints as well as GW constraints to a comparable space of parameters. Several electromagnetic observables tests have been conducted on its properties. We do want to mention that theories which do not belong to the Horndeski family, such as bigravity, non-local gravity, and generalised Proca theories, exhibit some of the same basic effects that we explore here, primarily adjustments to the GW luminosity distance. In particular, it was demonstrated that the fundamental parameter $\alpha_M$, which we described below in section 2.1, has analogues in the broader vector-tensor and tensor-tensor gravity theories.

We discuss a brief overview on the important features of Horndeski scalar-tensor theories in the context of gravitation, including their definition, the free functions that cover the related theory space, and how effectively these characteristics can be reflected at the level of the linearized action.

### 2.1 Horndeski Theories

The four-dimensional, Lorentz-invariant, local, energy-momentum conserving, and combination of equations of motion with second-order derivatives scalar-tensor theory of gravity is expressed in [8] as follows:

$$S[g_{\mu\nu},\phi] = \int d^4x\sqrt{-g}[\sum_{i=2}^{5}\frac{1}{8\pi G_N}\mathcal{L}_i[g_{\mu\nu},\phi]\mathcal{L}_m[g_{\mu\nu},\psi_m]] \tag{2.1}$$

$$\mathcal{L}_2 = G_2(\phi,X) \tag{2.2}$$

$$\mathcal{L}_3 = -G_3(\phi,X)\Delta\phi \tag{2.3}$$

$$\mathcal{L}_4 = G_4(\phi,X)R + G_{4X}(\phi,X)[(\delta\phi)^2 - \phi_{;\mu\nu}\phi^{;\mu\nu}] \tag{2.4}$$

$$\mathcal{L}_5 = G_5(\phi,X)G_{\mu\nu}\phi^{;\mu\nu} - 1/6G_{5X}(\phi,X)[(\delta\phi)^3 + 2\phi^{\ \nu}_{;\mu}\phi^{\ \alpha}_{;\nu}\phi^{\ \mu}_{;\alpha} - 3\phi_{;\mu\nu}\phi^{;\mu\nu}\delta\phi] \tag{2.5}$$

where the integration in $d^4x$ is carried out over the entire four-dimensional spacetime, R is the Ricci scalar, and $g = \det g_{\mu\nu}$. $G_i(\phi,X)$ is an arbitrary function of the extra scalar field, and $X = -\frac{1}{2}\Delta_\mu\phi\Delta^\mu\phi$ would be its kinetic term. The $G_i(\phi,X)$ functions and their partial derivatives determine the four values in the preceding equations. The Horndeski Lagrangian solely takes into account unified pairing between the metric and matter fields, which are separated from the scalar field and collectively characterised by m and primarily included in matter lagrangian L($\mathcal{L}_m$). The quitessence [9], k-essence [10, 11], kinetic gravity braiding[12], disformal and Dirac-Born-Indeld gravity[13]. are examples of model types that belong to the Horndeski class and further technical details is beyond the scope of this project.

We can now explain linear cosmic perturbations in terms of Horndeski gravity. The following line element would be used when dealing with linear scalar instabilities on a FRW metric, presuming spatial uniformity on massive scales, and using cosmic time t and comoving coordinates x, the line element would be:

$$ds^2 = -(1+2\frac{\phi}{c^2})c^2dt^2 + a^2(t)(1-2\frac{\psi}{c^2})dx^2 \tag{2.6}$$

The Bardeen potentials [14] and $\phi$ and $\psi$ fulfil the condition $\phi = \psi$ in General Relativity in the absence of anisotropic stress; however, in a modified gravity theory, this inclusiveness does not generally hold. We look into how linear cosmic disturbances are transformed in Horndeski gravity and constrain the background expansion using the ΛCDM. Only four functions of conformal time $\tau$ [15, 16] are required to factorise linear perturbations in Horndeski theories, which affect structure creation while mainly ignoring background expansion. For each of these four components, a coherent collection is crucial in terms of the physical biases connected to each one. For a detailed explanation of these four distinct roles which we can be refereed to [16] and here we briefly comment on their concise definition here: $\alpha_k$ defines the energy of the action-induced scalar instabilities. Since $\alpha_k$ does not enter the equations of motion in the quasi-static approximation, where time derivatives are negligible in comparison to space derivatives, we will set it to zero in our analysis; $\alpha_B$ is the braiding term, which describes the blending of the scalar field and the metric kinetic term. However, the dark energy component would only cluster on small levels if there is braiding, or when $\alpha_B = 0$ [17]; $\alpha_M$ is Planck Mass and is defined as $\alpha_M = \frac{d\ln M_*^2}{d\ln a}$, where the effective Planck mass, $M_*^2$, is defined as the non-dimensional product of a normalisation of the gravitons' kinetic term. $\alpha_M$ signifies the effective Planck mass' rate of evolution. Non-minimally connected theories have $\alpha_M \neq 0$, as shown by [18]. $\alpha_M$ **modifies the propagation of gravitational waves by producing anisotropic stress**; the gravitational wave propagation speed variations from the speed of light are indicated by the tensor speed, $\alpha_T$, which is defined as $c_T^2 = c^2[1+\alpha_T(z)]$. The value of $\alpha_T$ at this time has been constrained [1, 4, 19, 20] to be very close to zero by the measurement of the gravitational wave speed derived from the detection of the binary neutron star merger GW170817 and the associated gamma ray burst GRB170817A because the tensor speed was discovered to be extremely close to that of light. Although this limitation may not always be applicable to $\alpha_T$ values (see, for example,([13, 21]), defining $\alpha_T$ to disappear throughout all of cosmic history is the simplest choice.
We are thus left with three property functions, $\alpha_M$, $\alpha_B$, and $\alpha_K$, which cover the entire set of scalar-tensor theories compatible with the initial LIGO-Virgo GW detection. The background cosmic expansion rate must be independently set using the conventional CDM parameters and the dark energy equation of state, w(z), which we take to be $-1$ in this work. For a study that includes a modified expansion history, see [27, 28]. Since $\alpha_K$ is unaffected by large-scale structural probes and is not connected to any other factors, we fix it in our analysis. This usually leaves us with two Horndeski functions, $\alpha_M$ and $\alpha_B$, to constrain, but we only focus on constraining $\alpha_M$ parameter.

### 2.2 GW propagation in Horndeski Gravity

The system of equations of motion for tensor perturbations on a FRW background metric is used to examine the behaviour of cosmologically propagating GWs in reduction of Horndeski gravity. Given that many authors have already presented the derivations [22, 16], we may in fact present the resulting equation here:

$$h_A'' + [2 + \alpha_M(z)]\,\mathcal{H}h_A' + k^2 h_A = 0 \tag{2.7}$$

where A represents one of the two + and x GW polarizations, primes indicate conformal time derivatives, and $H = a'/a$ represents the conformal Hubble factor in the equation where h is a metric linear tensor perturbation. A large graviton, non-luminal GWs, and a quasi source of suitable anisotropic tension could all result in additional revisions to this equation in more general cases ([22, 21, 23]). Each of these effects involves more unusual types of GR deviations than is possible with merely the reduction of the Horndeski scalar-tensor class. The solution to equation 2.7 may then be expressed as $h_{MG,A} = \mathcal{C}h_{GR,A}$, where $h_{GR,A}$ stands for the GR solution for the amplitude. The luminosity distance $d_L$ is given by:

$$d_L = c(1+z)\int_0^z \frac{dz'}{H\,(z')} \tag{2.8}$$

where,

$$\Phi\,(\tau_{\rm obs}) = \Phi_0 - \left(\frac{5G_N\mathcal{M}_c(z)}{c^3}\right)^{-\frac{5}{8}} \tau_{\rm obs}^{\frac{5}{8}} \tag{2.9}$$

The resulting effective GW luminosity distance, $d_{GW}$, is given by:

$$d_{GW} = \mathcal{C}^{-1}d_L = d_L \exp\left[-\frac{1}{2}\int_0^x dx\alpha_M(x)\right] \tag{2.10}$$

Let's say the only electromagnetic redshift associated with a GW event is known. It is possible to detect the trace of modified gravity effects in the observable gap between the luminosity distance derived from the GW intensity and the reference redshift 2.10. A sequence of ten or more occurrences may be able to offer constraints on $\alpha_M(z)$ that are completely independent of current EM probes, even though the uncertainties on $d_{GW}$ assumed from signal amplitude are likely to be considerable for a single event. If the reader is interested in the complete mathematical derivation of the GW luminosity distance 2.10 from the 2.7 can refer to this paper [24] and the references within it. We consider the following ansatz [24] for this project;

$$\alpha_i(a) = \alpha_{i0}\Omega_\Lambda(a) \quad \text{and} \quad \alpha_i(a) = \alpha_{i0}a \tag{2.11}$$

$\alpha_{M0}$ and $\alpha_{B0}$ are the model's primary Horndeski parameters, and more information on these may be found here [24]. The two ansatz features in equation 2.11 are linearly growing functions that reduce to zero at greater gravitational redshifts and approach order unity at lower redshifts. These are all fundamental characteristics that deviations from GR are likely to have, which is why they are being used in this context. We stress that the two properties we just stated are only approximations that may allow our parameterized structure to catch the characteristics of some new physics; they are not totally derived from the fundamental theory. However, the approach described has been criticised in [25], hence we decided to focus on redshift as our only variable. The effectiveness of this method is seen in Figure 2.1, where several feasible models extending CDM (parametrized by $\alpha_M$ and $\alpha_B$) are displayed along with recent CMB and RSD data in the top panels. In particular, GW observations at high redshift are strongly inconsistent with ideas that cannot be confidently ruled out by the CMB and RSD data alone. This shows the possibility of GW standard siren data in the figure 2.2.

## 3 Methodology

For this study, we leverage the GW170817 and GW190521 [26] events to constrain gravity theories. GW190521 is unquestionably the merger that Advanced LIGO and Virgo [27, 28] detectors during O3 have detected at the greatest distance. Its luminosity distance is between 4 and 5 Gpc. An intermediate mass black hole was created when two black holes merged, which is how the discovery came to be. The potential EM equivalents associated with GW190521 at redshift $z = 0.438$ are $ZTF19abanrhr$ [29]. It is produced when two black holes in an AGN disc collide. By assuming that GW190521 and $ZTF19abanrhr$ are connected to roughly the very same astrophysical source, we can place constraints on modified theories of gravity.

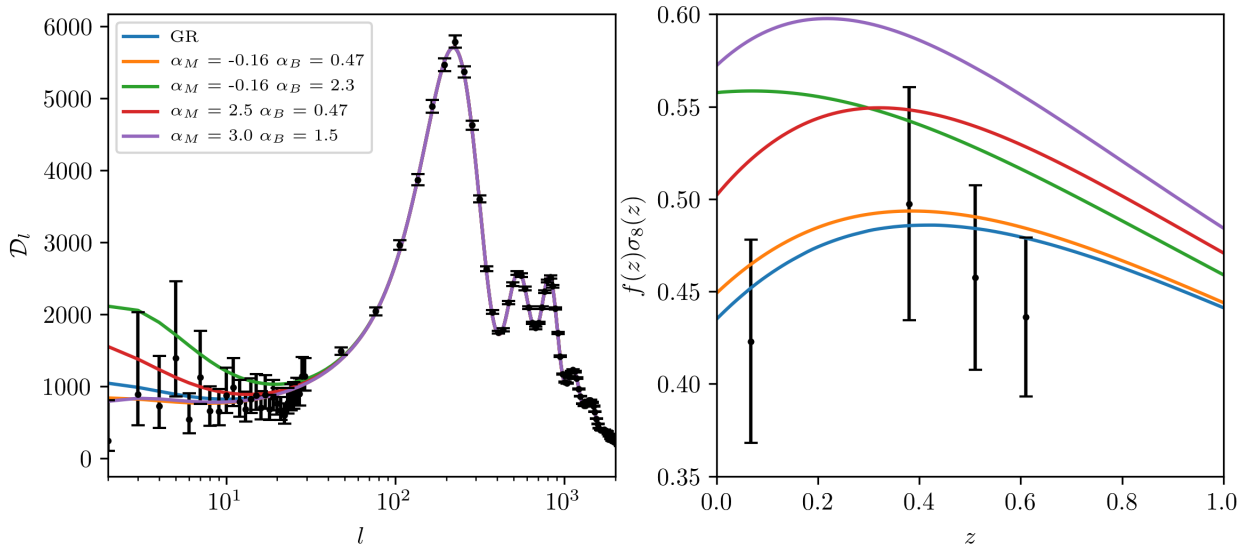


Figure 2.1: CMB power spectrum (left) and Redshift Space Distortion(right)

.

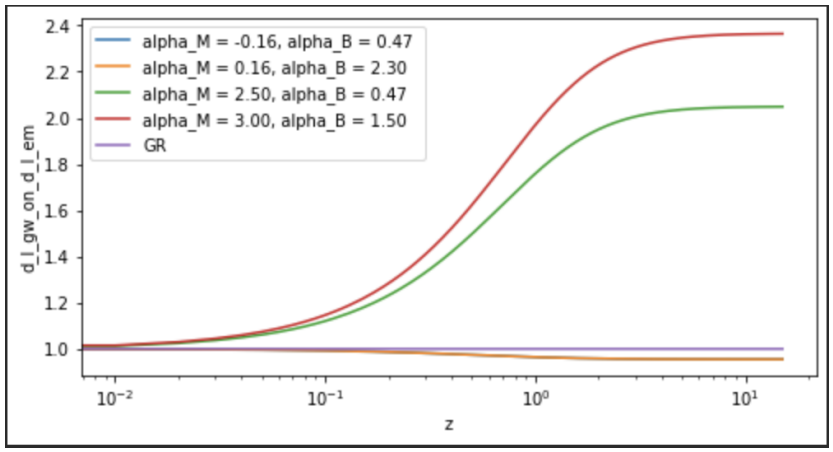


Figure 2.2: Comparison of the luminosity distance data used in this work. Section 2 goes into more information about theoretical curves, whereas Section 3 discuss data points.

.

## 3.1 Data

In conjunction to the gravitational wave data, we even incorporate restrictions from a pair of recent cosmology large scale data sets. This serves as context for the stricter constraints they offer for the $\alpha_M$ Horndeski parameter as well as additional constraints on cosmological parameters. They are the prime source of constraints for the $\alpha_B$ Horndeski parameter which do not influence the propagation of Gravitational Wvaes. Our technique and the data sets we used roughly correspond to [30] with the specified data sets discussed below, over the data from the CMB, RSd, and baryon acoustic oscillation, we generate the combined likelihood (BAO). All data sets are available as modules from the CosmoSIS standard library within a CosmoSIS pipeline.

### 3.1.1 CMB

We use the Planck 2015 Simple likelihood for CMB data. In particular, we employ the polarisation TT, EE, and TE data.

### 3.1.2 Redshift Space Distortions

We incorporate Redshift Space Distortion data from the 6dF Galaxy Survey and the DR12 agreement results of the Baryon Oscillation Spectroscopic Survey (BOSS) [31] , which constrain f(z)$\sigma_8$(z). As stated in section 2.2, it is crucial that the constraints from this data set only be used at a safe calibration scale where the growth rate is practically scale-independent when testing improved gravity models.

### 3.1.3 BAO

The volume averaged distance $D_V(z)$ is constrained by our BAO data, which come from WiggleZ [32], the SDSS MGS [33], and the consensus BOSS- DR12 results [31]. To restrict the cosmic parameters, we first execute an MCMC chain using only the CMB+RSD+BAO data sets (i.e., excluding GW data), to first check if the pipeline is estimating the correct results. Appendix A.3 contains information about the posteriors used and the posteriors acquired. The appendix A.2 cosmological parameter limitations for these Large scale structure (LSS)-only chains are in line with the earlier findings of [30]. The appendix A.1 contains the LSS including the gravitational wave data.

### 3.1.4 LIGO Data

We treat the gw170817 and gw190521 data, which were discovered by the Advanced LIGO-VIRGO (advLIGO) detector network, as standard sirens. These common sirens, which are produced by binary neutron star and a binary black hole mergers, come from a completely distinct population of mergers.

# 4 Theoretical Modelling

Using the real data described in section 3, we do a Monte Carlo analysis of the posterior probability distributions in order to get the best-fit values of the constraints on the cosmological and modified gravity parameters. We construct our pipeline using the modular CosmoSIS [34] cosmological parameter estimate algorithm, which enables us to establish a pipeline for calculating the required observables and sampling the parameter space. On the criteria that are considered before running the chains, we created broad priors.

## 4.1 Likelihood

The five data sets (CMB, RSD, BAO, LIGO GW) under discussion are assumed to be independent intuitively, and we assume a joint likelihood that may be divided into individual Gaussian likelihoods for each data set:

$$\mathcal{L}(D \mid \vec{\theta}) = \mathcal{L}\left(D_{\mathrm{CMB}} \mid \vec{\theta}\right) \mathcal{L}\left(D_{\mathrm{RSD}} \mid \vec{\theta}\right) \mathcal{L}\left(D_{\mathrm{BAO}} \mid \vec{\theta}\right) \mathcal{L}\left(D_{\mathrm{GW}} \mid \vec{\theta}\right) \tag{4.1}$$

where $\vec{\theta}$ is a vector holding all of the model parameters, $D_X$ is the data vector for each type of observable, and GW probability contains LIGO data. Each likelihood component for the CMB, RSD, and BAO sections using the real data vectors and covariance matrices offered in the CosmoSIS modules is a plain Gaussian. Using the best-fitting cosmology from the LSS-only runs, a diagonal covariance matrix for the GW parts of the LIGO data sets is employed using the methods in [24], with errors specified by the $\sigma_{dGW}$. Please note that, in contrast to our method here, [35] the whole information in the waveform using a Fisher matrix prediction..

## 4.2 Priors

Priors on the parameters utilised for this project's research are described in the table 4.1, along with parameter restrictions from recent Large Scale Structure data sets and the GW data. Priors of the type U(a,b) are uniform distributions on the range [a,b]. As a derived parameter, $\sigma_8$, a prior is not required.

## 4.3 Sampling

According to the posterior probability, we sample from this parameter space using the Markov Chain Monte Carlo ensemble sampler emcee [36]. An ensemble of 64 walkers is used to run chains across at least $10^5$ samples, 5000 of which are rejected for burn-in.

# 5 Results

The best-fit values and one-dimensional 68% confidence intervals for the posterior distributions depicted in fig 5.1 and are summarised in table 5.1. Below, we go over the Horndeski parameters' observed patterns. The entire posteriors for all of the parameters including both the ccosmological parameters and the Horndeski parameters from the available electromagnetic LSS-only data are displayed in Appendix A.3 and are remarkably compatible the previous findings from [30].

| **P**arameter | Prior | LSS-only $\propto \Omega_{DE}$ Constraint |
|---|---|---|
| $\Omega_m$ | $\mathcal{U}(0.1, 0.9)$ | 0.317316 |
| $h_0$ | $\mathcal{U}(0.55, 0.91)$ | 0.6849 |
| $\Omega_b$ | $\mathcal{U}(0.03, 0.12)$ | 0.0489 |
| $n_s$ | $\mathcal{U}(0.87, 1.07)$ | 0.968632 |
| $A_s$ | $\mathcal{U}(0.5 \times e^{-9}, 5.0 \times e^{-9})$ | 2.16325 $\times e^{-9}$ |
| $\tau$ | $\mathcal{U}(0.04, 0.125)$ | 0.0704925 |
| $\alpha_{B0}$ | $\mathcal{U}(-1, 3)$ | 1.03 |
| $\alpha_{M0}$ | $\mathcal{U}(-1, 6)$ | 0.473 |
| $\sigma_8$ | $--$ | 0.854164 |

Table 4.1: Priors

## 5.1 Constraints on the Parameters

The below figure 5.1 demonstrates the combined constraints on $\alpha_M$ and $\alpha_B$ for the propto-omega ansatze at $z = 0$. The contours provide a comparison of the relative constraining power provided by the EM data sets discussed in Section 3 when they are used alone(green) and in conjunction with both LIGO events (gw190521 and gw170817) (pink). The similar results has been produced for LSS with the inclusion of gw170817 gravitational wave data in [24]. As can be seen and inferred from the numbers in table 5.1. When compared to the findings of [24], the addition of LIGO data only modestly tightens the parameter restrictions for both models.

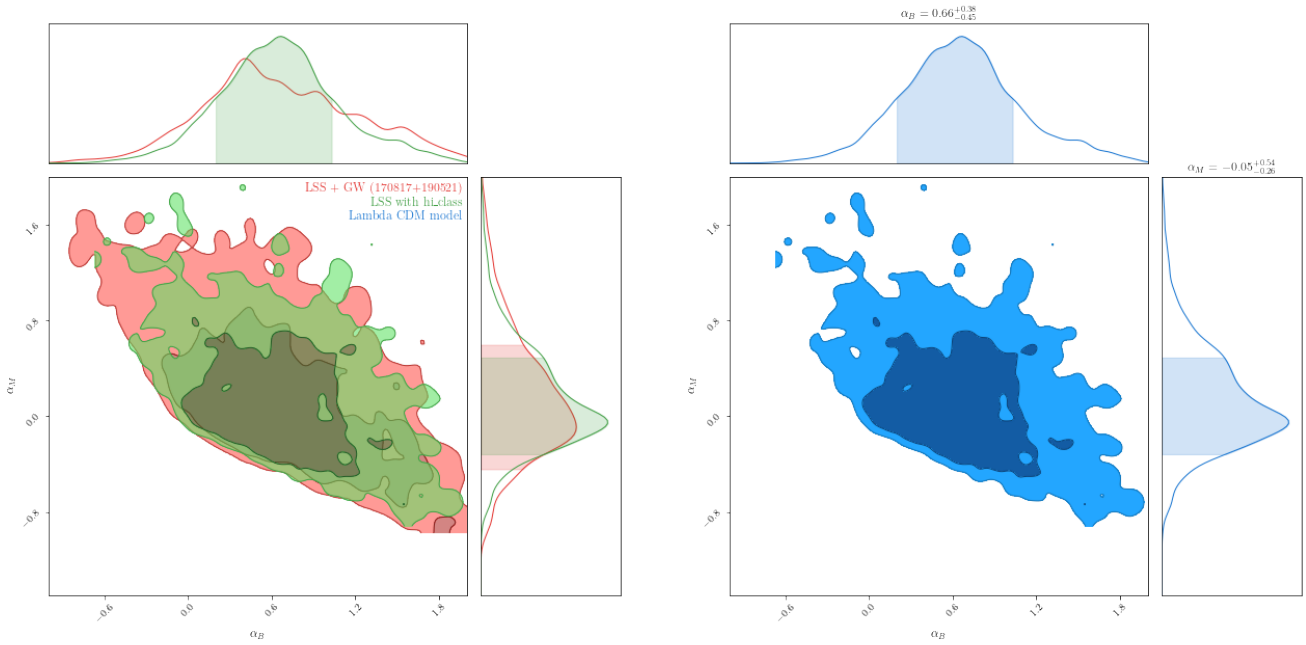


Figure 5.1: Limitations on coefficients that appear in both the $\propto \Omega_{DE}$, LSS plus GW data (left) and LSS with hi class (right) versions of the Horndeski $\alpha_M$ and $\alpha_B$ functions. The three sets of contours represent constraints from LSS with hi-class, LSS plus LIGO data, and ΛCDM, respectively.

## 5.2 Effect of Gravitational Wave Data

The expressions in section 2 make it clear that the luminosity distance of GW sources is only sensitive to the $\alpha_M$ parameter. The expressions in section 2 make it apparent that the $\alpha_M$ parameter is the sole one that affects how far away GW sources are from their observer. The contours which includes both the GW data sets in the figure 5.1 merely shrink vertically while remaining unchanged in $\alpha_B$ with the addition of GW data from LIGO. We can observe that LIGO events have relatively little constraining force since they primarily occur at low redshifts, where our cumulative departures from GR are quite small (see fig 2.2).

| Experiment | $\alpha_{MBO}$ | $\alpha_{MO}$ |
|---|---|---|
| LSS with hi-class | 0.836 | 0.333 |
| LSS+LIGO | 0.998 | 0.429 |

Table 5.1: Widths of one-dimensional Horndeski parameter with 68% confidence intervals.

### 5.3 Constraints on Large Scale Structure

Here, utilising the most recent Large Scale Structure surveys, we give the combined constraints on cosmological and Horndeski modified gravity parameters. Section 3 describes the data sets used in these restrictions, whereas Section 4 describes the anticipated likelihood and sampling. Table 4.1 displays the presumptions on the cosmological parameters. In addition, Table 5.1 displays the parameters' 68% confidence intervals and the best fit parameters, while Figures A.2 and A.3 display contour plots of the posteriors for the $\propto \Omega_{DE}$.

### 5.4 Software

Numerous software programmes, including NumPy, SciPy [37], Matplotlib [38], CosmoSIS [34], hi class [39], and IPython/Jupyter [40], were used to prepare this report. We employ ChainConsumer [41] for analysis and visualisation, and emcee [36] for sampling posterior distributions.

## 6 Conclusion and Future work

The direct observation of gravitational waves has led to a series of findings regarding the gravitational field in just seven years. The most important of them for cosmology may come from only two data point, GW170817 and GW190521. Our methodology has been quite conservative in many areas. The bounds in figure 5.1 do not predict that electromagnetic cosmic observables will get more precise in the future. Furthermore, we have restricted our research to changes in the GW amplitude caused by changes in GW luminosity distance. This is a highly general signature that modified gravity theories way outside the Horndeski class all share. However, modifications to the GW phase and post-Newtonian corrections are also feasible in alternative gravity models, and if they can be separated from the astrophysics of the source itself, they could offer equally useful limitations (such as spins of the MBHs). Although Horndeski gravity is coming under growing challenge on both the conceptual and methodological fronts [30, 42], it provides a great test case to show how EM and GW data complement each other. [24] showed that LISA standard sirens are only minimally sensitive to other important horndeski parameters, such as $\alpha_B$, but are able to improve the limits on some horndeski parameters by a factor of 7 over low-redshift data. Incorporating the large-scale structural data from DESI, Euclid, and the Vera Rubin Observatory [43] into our forecast is a logical extension of the current work. Due to the significance of modelling non-linear scales in modified gravity theories, our current forecast did not include the lensing data, but we note that other authors have formed constraints using approximate prescriptions [42], finding improvements by factors 1.5 over the LSS-only constraints are found here [24]. With the addition from the gravitational wave data detected from the LISA experiment a further better can be developed for the horndeski parameters which has been done in [24] where 50 mock GW data were simulated and tested against the available data. A part of which has been shown in the figure below 6.1

A series of neural cosmological power spectrum simulators can be created in order to speed up parameter estimation utilising two-point statistical analyses of the Large-Scale Structure (LSS) and Cosmic Microwave Background (CMB) surveys. The emulators don't need to be retrained for different choices of astrophysical parameters or redshift distributions since they do away with the need for Boltzmann codes to compute matter and CMB power spectra. The creation of a hi-class library emulator might be able to alleviate the memory leakage problem mentioned in 7.1 while computing the posteriors.

## 7 Critique of the Project

### 7.1 Execution phase

Figure 7.1 and 7.2 illustrates the various jobs and subtasks with the time they were planned to last and the time they took in the project's execution. It contrasts the initial project proposal with the actual project. While for the first few weeks before getting the access to the external machine the plan was to install the

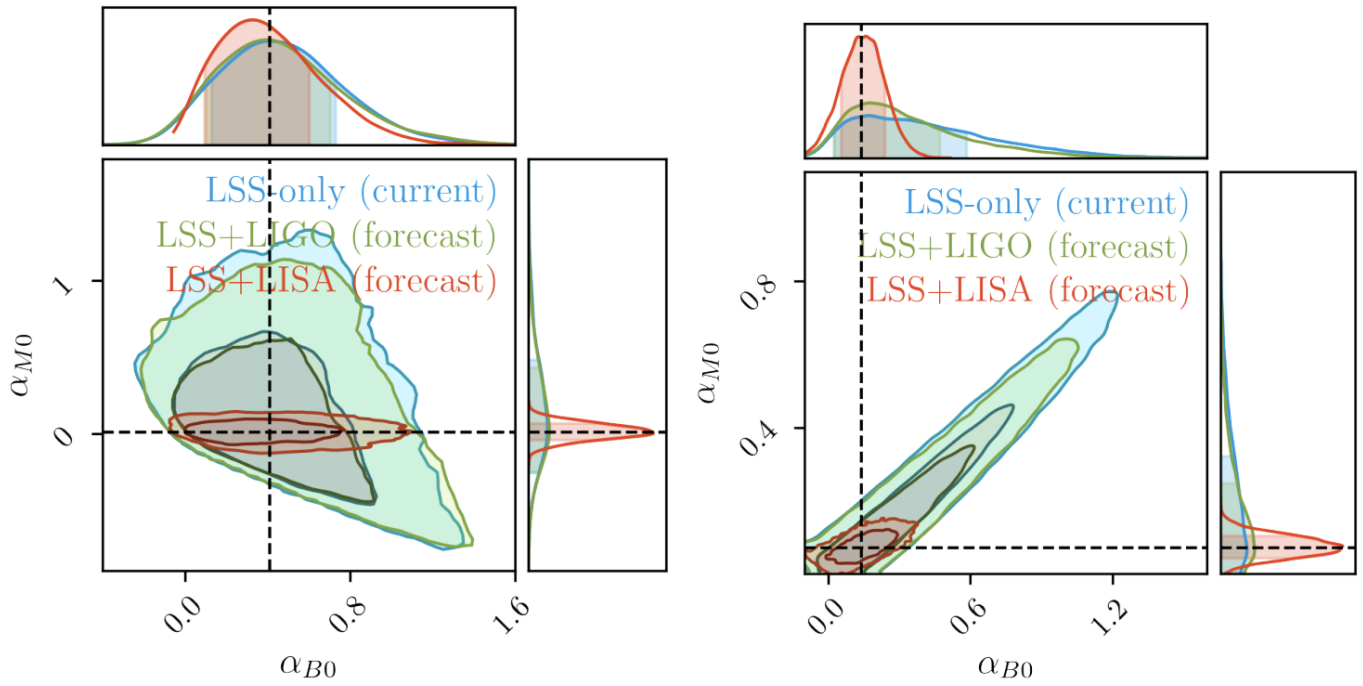


Figure 6.1: Constraints on $\alpha_M$ and $\alpha_B$ functions

.

| Week | 0 | 1 | 2 | 3 | 4 | 5 | 6 | 7 | 8 | 9 | 10 | 11 |
|---|---|---|---|---|---|---|---|---|---|---|---|---|
| Tasks | | | | | | | | | | | | |
| Join Darco | | | | | | | | | | | | |
| Familiarise with Cosmosis and Hi_class Libraries | | | | | | | | | | | | |
| Plot the ratio of d_GW/d_L | | | | | | | | | | | | |
| Running the MCMC chain | | | | | | | | | | | | |
| Building an emulator | | | | | | | | | | | | |
| Litreature review | | | | | | | | | | | | |
| Write first draft and get feedback | | | | | | | | | | | | |
| Revision final draft | | | | | | | | | | | | |
| Dissertation Submission | | | | | | | | | | | | |

Figure 7.1: Gantt chart for the proposed plan

.

| Week | 0 | 1 | 2 | 3 | 4 | 5 | 6 | 7 | 8 | 9 | 10 | 11 |
|---|---|---|---|---|---|---|---|---|---|---|---|---|
| Tasks | | | | | | | | | | | | |
| Join Darco | | | | | | | | | | | | |
| Familiarise with Cosmosis and Hi_class libraries | | | | | | | | | | | | |
| Plot the ratio of d_GW/d_L | | | | | | | | | | | | |
| Running the MCMC Chain | | | | | | | | | | | | |
| Litreature review | | | | | | | | | | | | |
| Write first draft and get feedback | | | | | | | | | | | | |
| Revision final draft | | | | | | | | | | | | |
| Dissertation Submission | | | | | | | | | | | | |

Figure 7.2: Gantt chart for the execution plan

.

CosmoSIS and hi-class library on my personal laptop (Apple M1 MacBook) and I was able to install the first library i.e CosmoSIS and when I moved to installing the hi-class library which is supposed to run on top of the CosmoSIS library, it was showing us a few errors and I realised the M1 architecture does not support the hi-class library and had to move the entire environment to the external machine (draco). The installation of the all the libraries was done on the external machine and the further environment was set up to do the further tasks.

The main thing that stands out among the proposed plan and the execution was running the MCMC chain. Plotting the ratio of the distance of gravitational wave source and the luminosity distance against the red-shift was fairly straightforward and did not consume time. While running the chain on the HPC (draco), I was facing the memory leakage issue on the hi-class pipeline mostly from the calculation of the gravitational wave

likelihood (hereafter, dgw) which was not apparent for the first time. Initially, I had tried to run the chains by removing the dgw likelihood from the pipeline and the problem would still persist, the chain would abruptly stop if the system memory is used at its full capacity and I had also received warnings from Richard Frewin several times as my script was crashing. The initial plan was to set up the environment and prepare the pipeline for running the mcmc chain by the end of week 3 which we have achieved. While me and Ian were trying figure out the leakage issue we had also thought of running the chains using the 4 cores of the draco machine which would produce the results in about three or four days and it was not feasible for us and we had opted for using 8 cores instead which had fastened the process by one and a half day. The cosmoSIS module had a feature of resuming the chains from where it had stopped earlier and using this method we started the desired results but it was very time consuming. This made us to re-think about concentrating on our last research question which was to build an emulator. We started getting our results by the week 6, which meant we were out of time for the next task and we decided to focus on this part. Although, we were able to proceed with the chains, I was trying to figure out the cause of the memory leakage and came up with some of the solutions and discussed it with Ian and we tried to implement it but unfortunately it was not working out and it was time consuming and we decided to leave out the part. Ian suggested a few changes in the dgw likelihhod calculation script and was not working out for us during that time. Naturally, building an emulator for the hi-class library would go on to the future scope of this project. Besides this, the results which we were able to produce on this research were a good learning tool as to how by varying the $\alpha_M$ has an effect in the gravitational wave luminosity distance as shown in fig 2.2. Figure 2.2 shows that, overall, although the project's initial stage went according to plan, flaws soon began to surface. Although this meant eliminating one of the objectives, it allowed for ensuring that the prior one was correctly accomplished. Since the following steps were always based on the previous outcomes, we were aware from the start that this project would require flexibility, but we made every effort to stick to the plan as closely as we could. But when we had to deviate from the plan, we did not hesitate, and in light of the project's outcomes, I think we made the right choices.

The literature review began a week before the project's scheduled start date and continued through to completion in order to enhance the summary and improve outcome inference. Every week, a respectable amount of time was set aside for the literature. The writing was supposed to start in week 3, however I started it in week 0 after summarising the literature précis from the proposal and implementing the feedback's suggested revisions. The methodology was written concurrently with the project's development, guaranteeing that even the smallest elements were included. Despite the fact that these were rough draft, it made writing much easier.

# 8 Bibliography

## References


[1] LIGO Scientific Collaboration and Virgo Collaboration *et al.* GW170817: Observation of Gravitational Waves from a Binary Neutron Star Inspiral. *Physical Review Letters* **119**, 161101 (2017). URL https://link.aps.org/doi/10.1103/PhysRevLett.119.161101. Publisher: American Physical Society.

[2] Collaboration, L. S. *et al.* Multi-messenger Observations of a Binary Neutron Star Merger. *The Astrophysical Journal* **848**, L12 (2017). URL http://arxiv.org/abs/1710.05833. ArXiv: 1710.05833.

[3] Mastrogiovanni, S., Steer, D. A. & Barsuglia, M. Joint tests of cosmology and modified gravity in light of GW170817. *arXiv:2004.06102 [astro-ph, physics:gr-qc]* (2020). URL http://arxiv.org/abs/2004.06102. ArXiv: 2004.06102.

[4] Baker, T. *et al.* Strong constraints on cosmological gravity from GW170817 and GRB 170817A (2017). URL https://arxiv.org/abs/1710.06394v1.

[5] Tasinato, G. Cosmic acceleration from Abelian symmetry breaking. *Journal of High Energy Physics* **2014**, 67 (2014). URL https://doi.org/10.1007/JHEP04(2014)067.

[6] Skordis, C. & Złośnik, T. Gravitational alternatives to dark matter with tensor mode speed equaling the speed of light. *Physical Review D* **100**, 104013 (2019). URL https://link.aps.org/doi/10.1103/PhysRevD.100.104013. Publisher: American Physical Society.

[7] Carroll, S. M., Sawicki, I., Silvestri, A. & Trodden, M. Modified-Source Gravity and Cosmological Structure Formation (2006). URL https://arxiv.org/abs/astro-ph/0607458v1.

[8] Horndeski, G. W. Second-order scalar-tensor field equations in a four-dimensional space. *International Journal of Theoretical Physics* **10**, 363–384 (1974). URL https://doi.org/10.1007/BF01807638.

[9] Ratra, B. & Peebles, P. J. E. Cosmological consequences of a rolling homogeneous scalar field. *Physical Review D* **37**, 3406–3427 (1988). URL https://link.aps.org/doi/10.1103/PhysRevD.37.3406. Publisher: American Physical Society.

[10] Armendáriz-Picón, C., Damour, T. & Mukhanov, V. k-Inflation. *Physics Letters B* **458**, 209–218 (1999). URL https://ui.adsabs.harvard.edu/abs/1999PhLB..458..209A. ADS Bibcode: 1999PhLB..458..209A.

[11] Armendariz-Picon, C., Mukhanov, V. & Steinhardt, P. J. Essentials of k-essence. *Physical Review D* **63**, 103510 (2001). URL https://ui.adsabs.harvard.edu/abs/2001PhRvD..63j3510A. ADS Bibcode: 2001PhRvD..63j3510A.

[12] Deffayet, C., Gao, X., Steer, D. A. & Zahariade, G. From $k$-essence to generalized Galileons. *Physical Review D* **84**, 064039 (2011). URL https://link.aps.org/doi/10.1103/PhysRevD.84.064039. Publisher: American Physical Society.

[13] de Rham, C. & Melville, S. Gravitational Rainbows: LIGO and Dark Energy at its Cutoff. *Physical Review Letters* **121**, 221101 (2018). URL http://arxiv.org/abs/1806.09417. ArXiv: 1806.09417.

[14] Uggla, C. & Wainwright, J. Cosmological Perturbation Theory Revisited. *Classical and Quantum Gravity* **28**, 175017 (2011). URL http://arxiv.org/abs/1102.5039. ArXiv: 1102.5039.

[15] Gleyzes, J., Langlois, D., Piazza, F. & Vernizzi, F. Essential building blocks of dark energy. *Journal of Cosmology and Astroparticle Physics* **2013**, 025–025 (2013). URL https://doi.org/10.1088/1475-7516/2013/08/025. Publisher: IOP Publishing.

[16] Bellini, E. & Sawicki, I. Maximal freedom at minimum cost: linear large-scale structure in general modifications of gravity (2014). URL https://arxiv.org/abs/1404.3713v3.

[17] Bellini, E., Cuesta, A. J., Jimenez, R. & Verde, L. Constraints on deviations from ${upLambda **2016**, 053–053 (2016). URL https://doi.org/10.1088/1475-7516/2016/02/053. Publisher: IOP Publishing.

[18] Saltas, I. D., Sawicki, I., Amendola, L. & Kunz, M. Anisotropic Stress as a Signature of Nonstandard Propagation of Gravitational Waves. *Physical Review Letters* **113**, 191101 (2014). URL https://link.aps.org/doi/10.1103/PhysRevLett.113.191101. Publisher: American Physical Society.

[19] Creminelli, P. & Vernizzi, F. Dark Energy after GW170817 and GRB170817A (2017). URL https://arxiv.org/abs/1710.05877v3.

[20] Sakstein, J. & Jain, B. Implications of the Neutron Star Merger GW170817 for Cosmological Scalar-Tensor Theories (2017). URL https://arxiv.org/abs/1710.05893v3.

[21] Amendola, L., Bettoni, D., Pinho, A. M. & Casas, S. Measuring Gravity at Cosmological Scales. *Universe* **6**, 20 (2020).

[22] Lagos, M., Bellini, E., Noller, J., Ferreira, P. G. & Baker, T. A general theory of linear cosmological perturbations: stability conditions, the quasistatic limit and dynamics. *Journal of Cosmology and Astroparticle Physics* **2018**, 021–021 (2018). URL https://doi.org/10.1088/1475-7516/2018/03/021. Publisher: IOP Publishing.

[23] Nishizawa, A. Generalized framework for testing gravity with gravitational-wave propagation. I. Formulation (2017). URL https://arxiv.org/abs/1710.04825v3.

[24] Baker, T. & Harrison, I. Constraining Scalar-Tensor Modified Gravity with Gravitational Waves and Large Scale Structure Surveys. *Journal of Cosmology and Astroparticle Physics* **2021**, 068–068 (2021). URL http://arxiv.org/abs/2007.13791. ArXiv: 2007.13791.

[25] Linder, E. V., Sengör, G. & Watson, S. Is the effective field theory of dark energy effective? *Journal of Cosmology and Astroparticle Physics* **2016**, 053–053 (2016). URL https://doi.org/10.1088/1475-7516/2016/05/053. Publisher: IOP Publishing.

[26] Multi-messenger Observations of a Binary Neutron Star Merger - NASA/ADS. URL https://ui.adsabs.harvard.edu/abs/2017ApJ...848L..12A/abstract.

[27] Aasi, a. J. *et al.* Advanced LIGO. *Classical and Quantum Gravity* **32**, 074001 (2015). URL https://doi.org/10.1088/0264-9381/32/7/074001. Publisher: IOP Publishing.

[28] Acernese, F. *et al.* Advanced Virgo: a second-generation interferometric gravitational wave detector. *Classical and Quantum Gravity* **32**, 024001 (2014). URL https://doi.org/10.1088/0264-9381/32/2/024001. Publisher: IOP Publishing.

[29] Graham, M. *et al.* Candidate Electromagnetic Counterpart to the Binary Black Hole Merger Gravitational-Wave Event S190521g. *Physical Review Letters* **124**, 251102 (2020). URL https://link.aps.org/doi/10.1103/PhysRevLett.124.251102. Publisher: American Physical Society.

[30] Noller, J. & Nicola, A. Cosmological parameter constraints for Horndeski scalar-tensor gravity. *Physical Review D* **99**, 103502 (2019). URL http://arxiv.org/abs/1811.12928. ArXiv:1811.12928 [astro-ph, physics:gr-qc, physics:hep-th].

[31] Alam, S. *et al.* The clustering of galaxies in the completed SDSS-III Baryon Oscillation Spectroscopic Survey: cosmological analysis of the DR12 galaxy sample. *Monthly Notices of the Royal Astronomical Society* **470**, 2617–2652 (2017). URL http://arxiv.org/abs/1607.03155. ArXiv:1607.03155 [astro-ph].

[32] Kazin, E. A. *et al.* The WiggleZ Dark Energy Survey: Improved Distance Measurements to z = 1 with Reconstruction of the Baryonic Acoustic Feature (2014). URL https://arxiv.org/abs/1401.0358v2.

[33] Ross, A. J. *et al.* The clustering of the SDSS DR7 main Galaxy sample – I. A 4 per cent distance measure at z = 0.15. *Monthly Notices of the Royal Astronomical Society* **449**, 835–847 (2015). URL https://doi.org/10.1093/mnras/stv154.

[34] Zuntz, J. *et al.* CosmoSIS: Modular cosmological parameter estimation. *Astronomy and Computing* **12**, 45–59 (2015). URL https://www.sciencedirect.com/science/article/pii/S2213133715000591.

[35] Tamanini, N. *et al.* Science with the space-based interferometer eLISA. III: Probing the expansion of the Universe using gravitational wave standard sirens. *Journal of Cosmology and Astroparticle Physics* **2016**, 002–002 (2016). URL http://arxiv.org/abs/1601.07112. ArXiv:1601.07112 [astro-ph, physics:gr-qc].

[36] Foreman-Mackey, D., Hogg, D. W., Lang, D. & Goodman, J. emcee: The MCMC Hammer (2012). URL https://arxiv.org/abs/1202.3665v4.

[37] Virtanen, P. *et al.* SciPy 1.0: fundamental algorithms for scientific computing in Python. *Nature Methods* **17**, 261–272 (2020). URL https://www.nature.com/articles/s41592-019-0686-2. Number: 3 Publisher: Nature Publishing Group.

[38] Hunter, J. D. Matplotlib: A 2D Graphics Environment. *Computing in Science & Engineering* **9**, 90–95 (2007). Conference Name: Computing in Science & Engineering.

[39] Zumalacarregui, M., Bellini, E., Sawicki, I., Lesgourgues, J. & Ferreira, P. G. hi_class: Horndeski in the Cosmic Linear Anisotropy Solving System (2016). URL https://arxiv.org/abs/1605.06102v2.

[40] Perez, F. & Granger, B. E. IPython: A System for Interactive Scientific Computing. *Computing in Science & Engineering* **9**, 21–29 (2007). Conference Name: Computing in Science & Engineering.

[41] Hinton, S. ChainConsumer. *Journal of Open Source Software* **1**, 45 (2016). URL https://joss.theoj.org/papers/10.21105/joss.00045.

[42] Spurio Mancini, A., Reischke, R., Pettorino, V., Schäfer, B. M. & Zumalacárregui, M. Testing (modified) gravity with 3D and tomographic cosmic shear. *Monthly Notices of the Royal Astronomical Society* **480**, 3725–3738 (2018). URL https://doi.org/10.1093/mnras/sty2092.

[43] Alonso, D., Bellini, E., Ferreira, P. & Zumalacárregui, M. Observational future of cosmological scalar-tensor theories. *Physical Review D* **95**, 063502 (2017). URL https://link.aps.org/doi/10.1103/PhysRevD.95.063502. Publisher: American Physical Society.

# A Appendix

## A.1 LSS with GW data Constraints

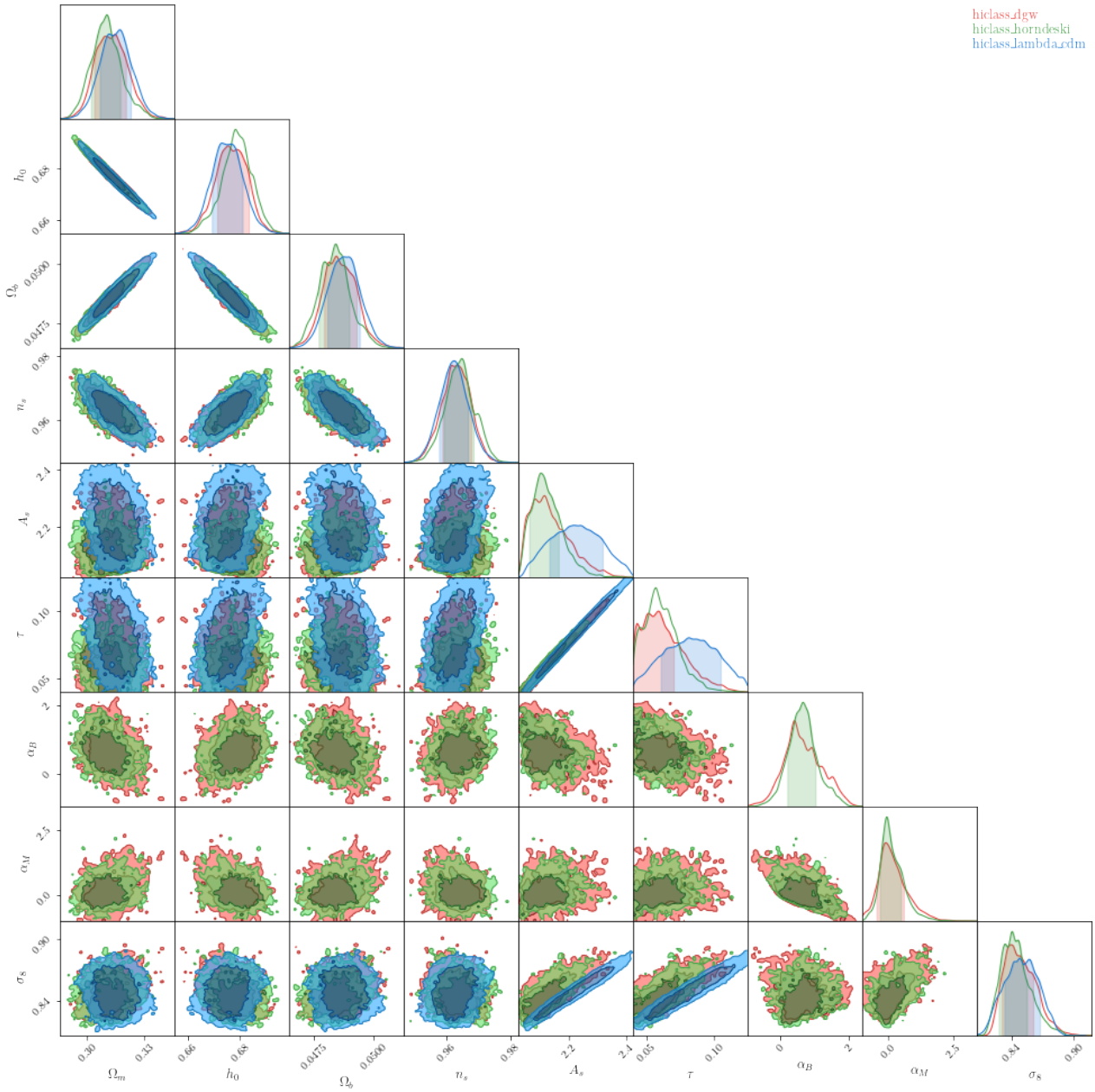


Figure A.1: Using the Large Scale Structure data sets and gravitational wave data sets provided in the text, constraints are imposed on cosmological and Horndeski parameters for the approach where $\propto \Omega_{DE}$

.

## A.2 LSS with Horndeski Parameters Constraints (excluding GW data)

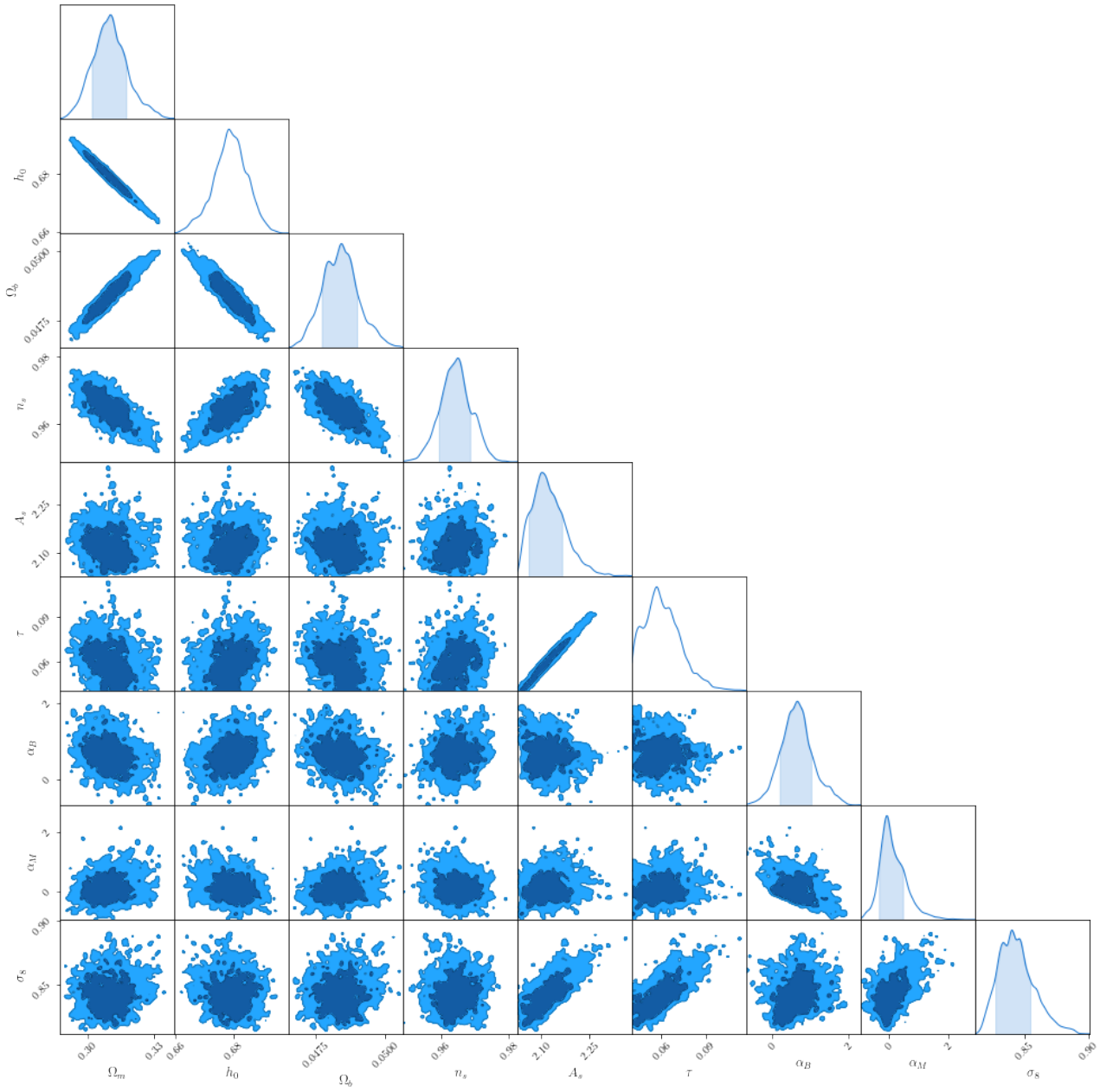


Figure A.2: Using the Large Scale Structure data sets provided in the text, constraints are imposed on cosmological and Horndeski parameters for the approach where $\propto \Omega_{DE}$

.

## A.3 LSS only Constraints

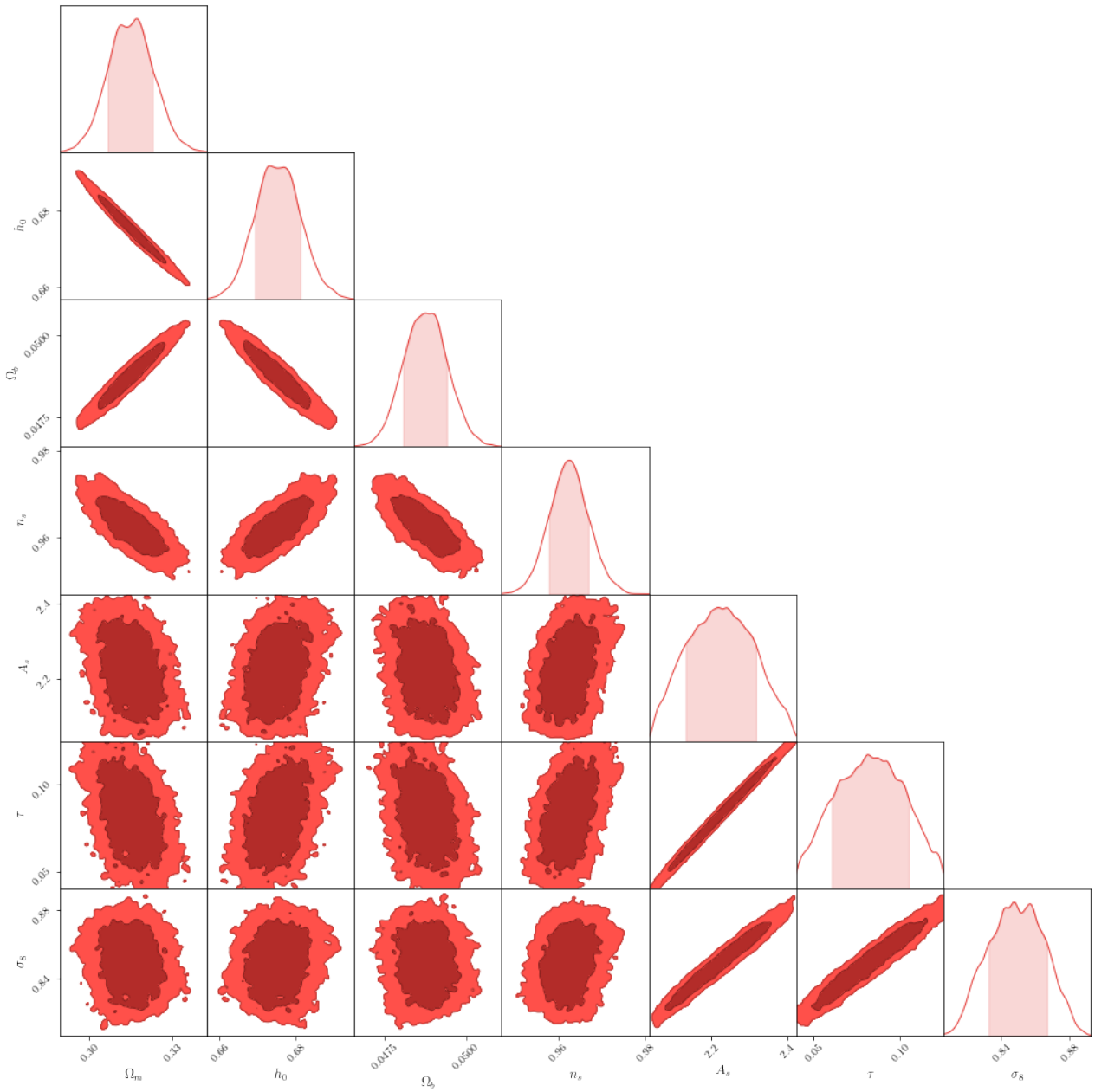


Figure A.3: LSS only without horndeski parameters

.